On the Borderline between *cis* and *trans* in Organometallic (Phosphane)platinum(II) Complexes

Dietrich Gudat,[a] Vimal K. Jain,[b] Axel Klein,*[c] Thilo Schurr,[c] and Stanislav Záliš[d]

Keywords: Density functional calculations / Isomers / NMR spectroscopy / Phosphane ligands / Platinum

The borderline between the *cis* and *trans* configurations in square-planar diarylplatinum(II) complexes with triethylphosphane ligands $[Pt(Ar)_2(PEt_3)_2]$ [Ar = 2,4,6-trimethylphenyl (mesityl), 2,6-dimethylphenyl, 2-methylphenyl, 3-methylphenyl, 4-methylphenyl and phenyl] has been investigated by a combination of multinuclear (^1H, ^{13}C, ^{31}P and ^{195}Pt) NMR spectroscopy, X-ray crystallography and quantum chemical (DFT) calculations. When formed under thermodynamic conditions, the complexes show a clear cut-off between *cis* (tolyl and phenyl complexes) and *trans* (2,6-xylyl and mesityl complexes). The *syn* and *anti* stereoisomers were identified for the 2-methylphenyl and 3-methylphenyl derivatives. Calculated data (structural isomers or NMR) are in excellent agreement with experimental findings.

Introduction

The stability of the *cis* or *trans* conformation of square-planar complexes with a d^8 configuration is usually governed by an interplay of steric and electronic factors:[1,2] bulky ligands tend to avoid each other, and the presence of two of them usually leads to a *trans* configuration, whereas strong donor ligands prefer a *cis* orientation towards other strong ligands due to the *trans* influence. The latter should not be confused with the *trans* effect. The former is responsible for ground state-properties (structure, thermodynamic stability etc.), whereas the latter governs the behaviour in chemical reactions.[1] Both the *trans* influence and the *trans* effect are of high importance since both stability and formation reactions predetermine the occurrence of *cis* and *trans* configurations in such complexes, which is very often crucial for their applications. This is of enhanced importance for platinum(II) complexes, since in the series of d^8-configured transition metals like Rh^I, Ir^I, Ni^{II}, Pd^{II}, Pt^{II} and Au^{III} platinum(II) derivatives are markedly more resistant to isomerisation reactions than others.[1–3] The most prominent example of the different behaviour of two isomeric platinum(II) complexes is probably diamminedichloroplatinum $[PtCl_2(NH_3)_2]$: the *cis* derivative is an effective anti-cancer drug ("cisplatin") with sales of around 2 million € a year, whereas the *trans* derivative is inactive in that respect.[4–6]

Phosphane ligands have been explored in organoplatinum complexes for more than half a century.[2,7–9] Besides their numerous applications in organometallic catalysis, they have been found to be ideally suited for the determination of their configurations or configurational equilibria since the ^{31}P–^{195}Pt coupling constants are very sensitive to the *trans* and *cis* influence of further co-ligands.[10,11] Aryl ligands can be used to probe the subtle interplay of steric and electronic factors of the configuration since they are (i) strongly donating ligands; (ii) their electronic properties can be tuned by various substituents and the observed changes can be easily rationalised in terms of inductive or mesomeric influences; (iii) they can be easily introduced by established metathesis reactions;[9] (iv) their steric demand can be varied almost deliberately;[12] and (v) since their ring planes are usually oriented almost perpendicular with respect to the binding plane they allow discrimination of the two hemispheres above and below the binding plane, for example by unsymmetrical aryl ligands like 2-R,6-R′-C_6H_4 that give rise to further isomerism.[13]

We therefore decided to prepare a series of (triethylphosphane)platinum complexes $[Pt(Ar)_2(PEt_3)_2]$ [Ar = 2,4,6-trimethylphenyl (Mes), 2,6-dimethylphenyl (Xyl), 2-methylphenyl (2-Tol), 3-methylphenyl (3-Tol), 4-methylphenyl (4-Tol) and phenyl (Ph)] with various alkyl substitution patterns on the aryl ligands.

A similar study was undertaken by Rieger and coworkers some years ago[14] and some of the compounds (Ar = Ph, 2-Tol, 4-Tol) were reported in 1959 by Chatt and Shaw.[9] However, their preparation routes, involving me-

[a] Institut für Anorganische Chemie, Universität Stuttgart, Pfaffenwaldring 55, 70569 Stuttgart, Germany
E-mail: gudat@iac.uni-stuttgart.de
[b] Novel Materials and Structural Chemistry Division, Bhabha Atomic Research Centre, Mumbai 400 085, India
E-mail: jainvk@apsara.barc.ernet.in
[c] Institut für Anorganische Chemie, Universität zu Köln, Greinstraße 6, 50939 Köln, Germany
E-mail: axel.klein@uni-koeln.de
[d] J. Heyrovsky Institute of Physical Chemistry, Academy of Sciences of the Czech Republic, Dolejškova 3, 18 000 Prague 8, Czech Republic
E-mail: stanislav.zalis@jh-inst.cas.cz

  DOI: 10.1002/ejic.200500251

tathesis reactions between *cis*- or *trans*-[$PtCl_2(PEt_3)$] and an appropriate Grignard reagent, did not allow synthesis of the sterically highly crowded dimesityl or bis(2,6-xylyl) derivatives and often led to mixtures of isomers.[9,14] To prevent this we have chosen a different preparation route to ensure the thermodynamically controlled selective formation of only one isomer. To this end we applied ligand-exchange reactions at elevated temperatures using the DMSO precursor complexes [$Pt(Ar)_2(DMSO)_2$] to obtain isomerically pure compounds.

Results and Discussion

Preparation

The preparation of the complexes was performed as shown in Scheme 1 from the corresponding DMSO derivatives [$Pt(Ar)_2(DMSO)_2$][15] by ligand-exchange reactions at elevated temperatures (boiling toluene, see Exp. Sect.). With the exception of [$Pt(2\text{-Tol})_2(PEt_3)_2$], where ^1H and ^{31}P NMR spectra showed the presence of two isomers, we observed in all cases the formation of only one isomer in the crude reaction product as well as in the recrystallised products.

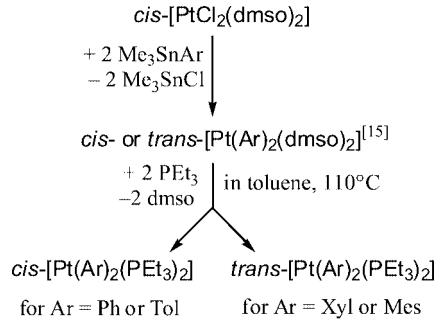

Scheme 1. Preparation of the platinum complexes [$Pt(Ar)_2(PEt_3)_2$].

NMR Spectroscopy

The thoroughly recrystallised complexes were submitted to multinuclear (^1H, ^{13}C, ^{31}P and ^{195}Pt) NMR studies. Selected data for the determination of the structure by NMR spectroscopy are summarised in Table 1 together with ADF/BP calculated data. Full NMR spectroscopic data can be found in the Experimental Section.

From the NMR spectroscopic data, especially from the $^1J_{Pt,P}$ and $^1J_{Pt,C(1)}$ coupling constants (Table 1), a clear line can be drawn between the Ph and Tol derivatives on one side and the Xyl and Mes derivatives on the other side. The $^1J_{Pt,P}$ coupling constants of the former are markedly smaller and the $^1J_{Pt,C(1)}$ couplings markedly larger than the values found for the more substituted derivatives. Both findings are indicative of shorter Pt–P and longer Pt–C(1) bonds, and thus the less substituted derivatives are assigned to have *cis* configurations whereas the more substituted ones are *trans*-configured. The calculated $^1J_{Pt,C}$ coupling constants are in excellent agreement with the experimental ones and clearly support the assignment of *cis* and *trans* configurations. Due to the simplification of the phosphane ligand (PMe_3 instead of PEt_3), the calculated $^1J_{Pt,P}$ coupling constants reflect the *cis*/*trans* variation only qualitatively.

Two sets of signals (ca. 2:1 ratio) were found for the 2-Tol derivative (Figure 1), both clearly showing a *cis* configuration. The two isomers correspond to species with a *syn* (C_S symmetry) and *anti* (C_2 symmetry) orientation of the two *ortho*-methyl groups (above and below the coordination plane), as has been reported previously for these systems[14] and related ditolyl complexes.[16,17] Detailed NMR experiments, including ^1H gsNOESY, ^1H,^{13}C HMQC and ^1H,^{195}Pt HMQC experiments, allowed the assignment of all signals to the two stereoisomers. Furthermore, the absence of exchange correlations in the ^1H NOESY spectra disclosed that the stereoisomers do not undergo any mutual exchange on a second time-scale, even in the presence of additional PEt_3. This stands in contrast to similar results

Table 1. Experimental[a] and calculated (DFT)[b] NMR spectroscopic data for complexes [$Pt(Ar)_2(PEt_3)_2$].

Ar	$^1J_{Pt,C(1)}$ exp. [Hz]	$^1J_{Pt,C}$ calcd. [Hz]	$^1J_{Pt,P}$[c] exp. [Hz]	$^1J_{Pt,P}$ calcd. [Hz]	$\delta_{^{195}Pt}$ [ppm]	Conformation from NMR spectroscopic data
Ph	879	*cis*: 840.1 *trans*: 512.1	1775	*cis*: 1093.8 *trans*: 2575.3	–4568	*cis*
2-Tol (*syn*)	844	*cis*: 888.8 *trans*: 541.6	1751	*cis*: 942.2 *trans*: 2566.8	–4471	*cis-syn*
2-Tol (*anti*)	832	*cis*: 874.7 *trans*: 514.8	1739	*cis*: 933.9 *trans*: 2566.9	–4466	*cis-anti*
3-Tol	812	*cis*: 856.0 *trans*: 537.6	1754	*cis*:1005.8 *trans*: 2455.4	–4570	*cis*
4-Tol	1090	*cis*: 846.7 *trans*: 517.8	1762	*cis*: 959.8 *trans*: 2346.9	–4566	*cis*
Xyl	591	*cis*: 937.4 *trans*: 526.8	2835	*cis*: 985.1 *trans*: 2595.5	–4311	*trans*
Mes	536	*cis*: 922.7 *trans*: 530.2	2841	*cis*: 875.1 *trans*: 2737.8	–4306	*trans*

[a] As measured in $CDCl_3$ at 303 K. [b] Calculated for [$Pt(Ar)_2(PMe_3)_2$]. [c] From ^{31}P NMR measurements.

with the related DMSO complexes *cis*-[Pt(2-Tol)$_2$(DMSO)$_2$], where *syn*/*anti* isomerisation takes place presumably by a dissociative pathway.[15] Analogous stereoisomers were expected for the 3-Tol derivative. However, we found only one set of signals in the NMR spectra at ambient temperature (298 K). Recently, Hashemi and Rashidi have reported line-broadening on related bis(3-Tol) and bis(4-Tol) complexes, thus indicating fluxional behaviour.[16] We therefore performed quantum-chemical calculations on the energy barrier of *syn*/*anti* isomerisation of the 2-Tol and 3-Tol derivatives. The barrier calculated for [Pt(2-Tol)$_2$(PMe$_3$)$_2$] (111.7 kcal mol^{-1}) turns out to be much larger than for [Pt(3-Tol)$_2$(PMe$_3$)$_2$] (34.1 kcal mol^{-1}), which seems to be reasonable. However, both numbers indicate the occurrence of *syn* and *anti* isomers for 2-Tol as well as for 3-Tol. We therefore examined the 3-Tol derivative at low temperatures (223 and 193 K) and found two sets of signals in the ^{1}H, ^{13}C, ^{31}P and ^{195}Pt NMR spectra. Due to the rather small splitting of the corresponding signals of the two isomers (some signals are just broadened; see, for example, Tables 6 and 7) and signal ratios of approximately 1:1, we could not assign either the *syn* or *anti* isomers or calculate the energy difference. We also refrained from measuring exact coalescence temperatures since the two measurements (at 223 and 193 K) indicated already that different coalescence temperatures will be found for the various signals.

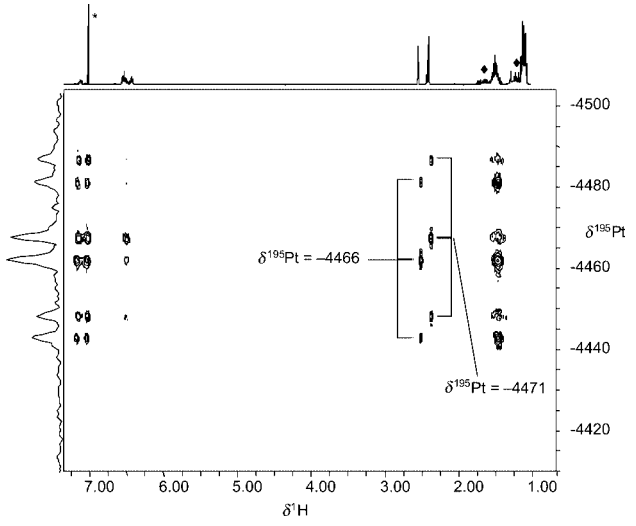

Figure 1. Magnitude-mode two-dimensional ^{1}H,^{195}Pt gs-HMQC spectrum (defocusing time 8.3 ms), showing various long-range correlations between the protons in the 2-Tol and PEt$_3$ groups and the metal atom, and the ^{1}H NMR spectrum (top projection; the solvent signal is denoted by * and the resonances of an impurity of OPEt$_3$ by ♦) of a mixture of the *syn* and *anti* stereoisomers of *cis*-[Pt(2-Tol)$_2$(PEt$_3$)$_2$]. The *F*1 projection (left) shows the ^{195}Pt signals of both isomers as interleaved triplets split by $^1J_{Pt,P}$.

Comparing the *syn*/*anti* ratios for the 2-Tol and 3-Tol derivatives we found a ratio of approx. 1:1 for 3-Tol, whereas for the 2-Tol derivative the ratio is about 2:1. This ratio is reversed (*syn*/*anti* = 1:2) in the precursor complex *cis*-[Pt(2-Tol)$_2$(DMSO)$_2$].[15] Since for the DMSO derivative we found isomerisation already at ambient temperature (NMR), we assume that the *syn* derivative of the DMSO precursor complex is more reactive than the *anti*, which is (thermodynamically) slightly more stable. It is also worthwhile mentioning that the PEt$_3$ complexes retain the *cis* or

Table 2. Crystallographic and structure refinement data of complexes [(PEt$_3$)$_2$Pt(Ar)$_2$].[a]

Ar	Ph (*cis*)	3-Tol (*cis*)	4-Tol (*cis*)	Xyl (*trans*)	Mes (*trans*)
Empirical formula	$C_{24}H_{40}P_2Pt$	$C_{26}H_{44}P_2Pt$	$C_{26}H_{44}P_2Pt$	$C_{28}H_{48}P_2Pt$	$C_{30}H_{52}P_2Pt$
Formula mass	585.59	613.64	613.64	641.69	669.75
Crystal system	monoclinic	monoclinic	monoclinic	triclinic	orthorhombic
Space group	*Cc*	$P2_1/c$	$P2_1/n$	$P\bar{1}$	$Pca2_1$
a [Å]	20.411(5)	15.951(3)	13.3174(15)	8.8835(18)	22.885(5)
b [Å]	9.8288(14)	10.111(2)	14.8753(19)	10.314(2)	9.2381(18)
c [Å]	15.3942(17)	17.737(4)	14.5993(18)	15.804(3)	14.246(3)
α [°]	90	90	90	90.54(3)	90
β [°]	124.411(13)	104.37(3)	99.662(9)	91.09(3)	90
γ [°]	90	90	90	104.44(3)	90
V [Å^3]	2547.9(7)	2771.1(10)	2851.1(6)	1401.9(5)	3011.8(10)
Z	4	4	2	2	4
$\rho_{calcd.}$ [g cm^{-3}]	1.527	1.471	1.430	1.520	1.477
μ [mm^{-1}]/*F*(000)	5.639/1168	5.189/1232	5.043/1232	5.132/648	4.781/1360
Limiting indices	$0 \le h \le 27$	$-17 \le h \le 20$	$0 \le h \le 17$	$-10 \le h \le 11$	$-1 \le h \le 30$
	$0 \le k \le 13$	$-8 \le k \le 13$	$0 \le k \le 19$	$-13 \le k \le 13$	$-1 \le k \le 12$
	$-21 \le l \le 17$	$-23 \le l \le 22$	$-18 \le l \le 18$	$-20 \le l \le 20$	$-1 \le l \le 18$
Reflections collected/unique	3463/3463	6596/6371	6423/6162	7200/6769	4718/4054
R_{int}	0.0639	0.0614	0.0460	0.0388	0.0369
Data/restraints/parameters	3463/2/250	6371/11/306	6160/0/270	6769/0/293	4054/1/322
Goof. on F^2	1.031	1.050	1.007	1.179	1.212
Final indices: R_1	0.0323	0.0691	0.0650	0.0295	0.0364
$[I > 2\sigma(I)]$ wR_2	0.0730	0.1425	0.1326	0.0824	0.0758
R value all data: R_1	0.0417	0.1270	0.1416	0.0398	0.0528
wR_2	0.0769	0.1718	0.1617	0.0919	0.0822
Largest diff. peak/hole [e Å^{-3}]	1.505/–1.427	1.976/–2.538	3.419/–2.313	1.122/–1.445	1.378/–1.069

[a] Measurement temperature: 173(2) K; radiation wavelength: 0.71073 Å; refinement method: full-matrix least squares on F^2; absorption correction: empirical, ψ-scans.

trans configuration of their DMSO precursors. This is not trivial, since the DMSO precursor complexes may undergo facile isomerisation, which comprises not only *syn*/*anti* (vide supra) but also *cis*/*trans* isomerisation, for example during the formation of the *cis*-configured (diimine)platinum complexes *cis*-[Pt(Ar)$_2$($\widehat{NN}$)] ($\widehat{NN}$ = α-diimine; Ar = Mes or Xyl) from *trans*-configured DMSO precursor complexes.[18–20]

Crystal Structures

The crystal and molecular structures of [Pt(Ph)$_2$(PEt$_3$)$_2$], [Pt(3-Tol)$_2$(PEt$_3$)$_2$], [Pt(4-Tol)$_2$(PEt$_3$)$_2$], [Pt(Xyl)$_2$(PEt$_3$)$_2$] and [Pt(Mes)$_2$(PEt$_3$)$_2$] were determined from single-crystal XRD experiments. The structures of the *syn* and *anti* isomers of *cis*-[Pt(2-Tol)$_2$(PEt$_3$)$_2$] have been reported previously by Rieger et al.[14] The results of the structure determinations are summarised in Table 2, with bond lengths and angles given in Table 3. The first three compounds crystallise in monoclinic space groups, the Xyl derivative is found in triclinic $P\bar{1}$ and the Mes compound in orthorhombic $Pca2_1$. No significant intermolecular contacts were found in any of the crystal structures.

The molecular structures confirm the conclusions drawn from spectroscopic studies in solution: The Ph, 3-Tol and 4-Tol derivatives exhibit a *cis* conformation (Figure 2) as has been found before for the 2-Tol derivative.[14] The Xyl and Mes derivatives show a *trans* orientation of the two aryl groups (Figure 3), and the platinum atom lies on a centre of symmetry for Ar = Xyl. The 3-Tol derivative shows a *syn* orientation of the two methyl substituents. All structures show nearly perfect planar arrangements of ligands around the platinum atom, as can be seen from the sum of angles and the small CCPt/PPPt tilt angles (Table 3).

The bond lengths and angles around the platinum atom in the series of complexes nicely reflect the *trans* influence.[1] For instance, the Pt–P distances are slightly longer for the *cis*-configured compounds while the Pt–C distances are markedly shorter. The bond lengths and angles of the previously reported *syn* and *anti* isomers of *cis*-[Pt(2-Tol)$_2$(PEt$_3$)$_2$][14] fit nicely into our series. Interestingly, Osakada et al.[21] have recently reported the structure of the *trans*-

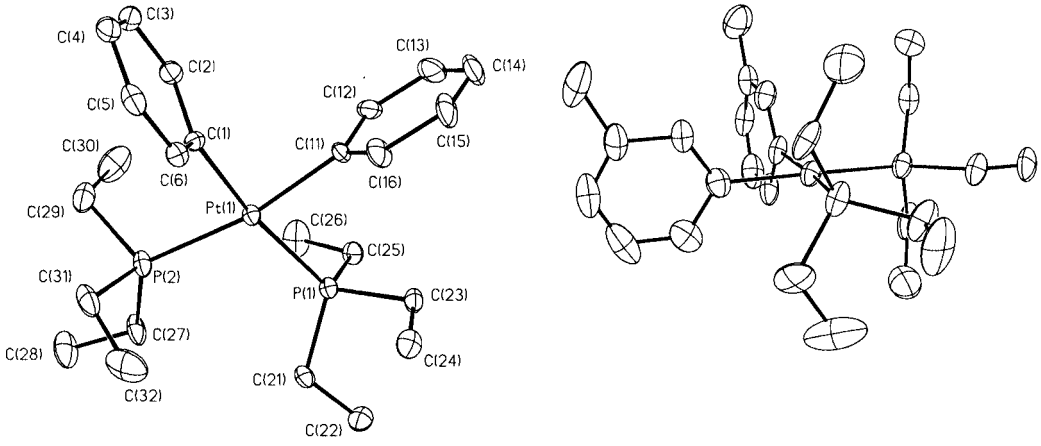

Figure 2. Molecular structures (30% thermal ellipsoids) of *cis*-[(Pt(Ar)$_2$(PEt$_3$)$_2$] with Ar = Ph (left, with full numbering) and 3-Tol (right). H atoms omitted for clarity.

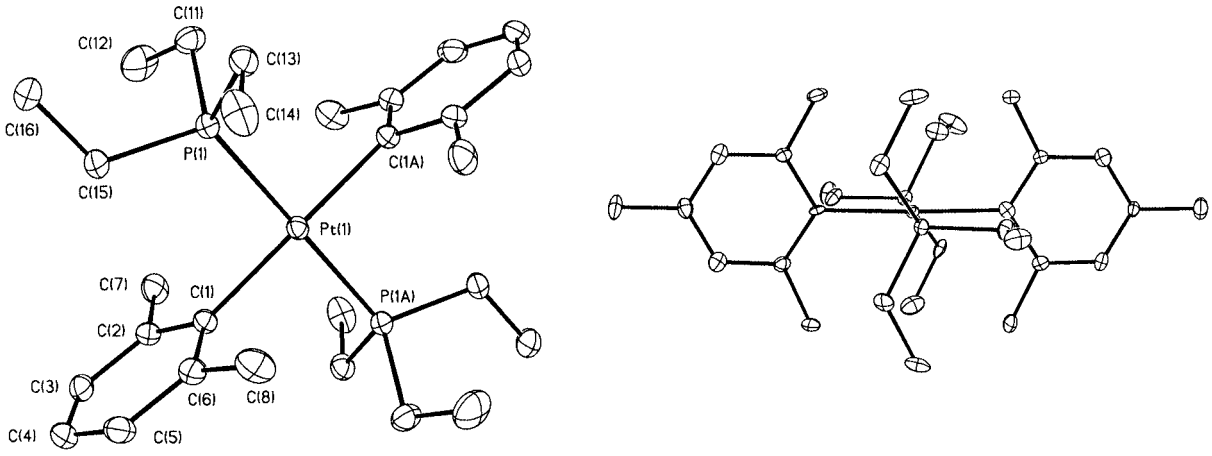

Figure 3. Molecular structures (30% thermal ellipsoids) of *trans*-[(Pt(Ar)$_2$(PEt$_3$)$_2$] with Ar = Xyl (left) or Mes (right). H atoms omitted for clarity.

Table 3. Selected bond lengths [Å] and bond angles [°] of complexes $[(PEt_3)_2Pt(Ar)_2]$.[a]

	Ph (*cis*)	4-Tol (*cis*)	3-Tol (*cis*)	Xyl (*trans*) (1)[b]	Xyl (*trans*) (2)[b]	Mes (*trans*)
Pt–P(1)	2.318(2)	2.309(3)	2.301(3)	2.2991(12)	2.2954(13)	2.296(2)
Pt–P(2)	2.328(2)	2.324(4)	2.316(3)	2.2991(12)	2.2954(13)	2.290(2)
Pt–C(1)	2.061(9)	2.057(12)	2.067(12)	2.113(4)	2.104(3)	2.101(8)
Pt–C(11)	2.073(8)	2.057(9)	2.083(11)	2.113(4)	2.104(3)	2.104(7)
Pt–C(7/17)	–	–	–	3.346(5)	3.360(4)	3.319(7), 3.375(7)
Pt–C(8/18)	–	–	–	3.377(5)	3.367(3)	3.336(8), 3.377(8)
P–Pt–P	103.72(8)	99.32(11)	102.12(11)	180.00(7)	180.00(6)	179.66(10)
C–Pt–C	84.3(3)	83.4(4)	84.2(5)	180.0(3)	180.0(2)	178.1(6)
C(1)–Pt–P(1)	86.2(2)	90.2(3)	88.3(3)	90.45(11)	91.58(10)	90.5(2)
C(1)–Pt–P(2)	169.1(2)	170.2(3)	169.1(3)	89.55(11)	88.42(10)	89.7(2)
C(11)–Pt–P(2)	86.3(2)	87.3(3)	85.6(3)	90.45(11)	91.58(10)	90.7(3)
C(11)–Pt–P(1)	169.1(2)	172.4(4)	171.8(3)	89.55(11)	88.42(10)	89.1(3)
Sum of angles	360.52	360.22	360.22	360.00	360.00	360.00
Tilt CCPt/PPPt	6.7	4.8	4.5	0.00 [c]	0.00 [c]	1.9 [c]
CCPtPP/aryl	86.0, 76.3	89.9, 83.4	80.3, 86.6	89.3	88.7	85.5, 89.9

[a] Numbering scheme employed in figures and text is as shown in Scheme 2. [b] Two molecules (1) and (2) were found for Ar = Xyl, each with a centre of inversion on the platinum atom. [c] Tilt angles PCPt/PCPt.

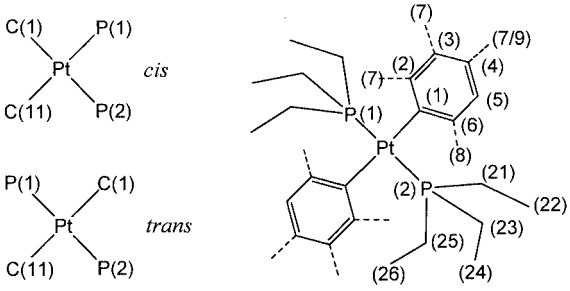

Scheme 2. Numbering scheme.

configured complex $[Pt(4\text{-}CF_3Ph)_2(PEt_3)_2]$, which they obtained by an oxidative addition/reductive elimination sequence using $[PtBr(PEt_3)_3]BF_4$ and the silanol 4-$CF_3PhSi(Me)_2OH$. The Pt–C bonds are markedly longer [2.089(8) Å] and the Pt–P bonds slightly shorter [2.287(3) Å] than what we found for the *cis*-4-Tol derivative.

The distances between the *ortho*-methyl groups and the platinum atoms in compounds Ar = Xyl or Mes range from 3.32 to 3.38 Å, with the upper value representing approximately the sum of the van der Waals radii of Pt and CH_3,[17] values which have also been found for the series of phosphane(2-Tol)platinum complexes reported by Rieger et al.[14] They are slightly lower for the (diimine)platinum complexes *cis*-$[Pt(Ar)_2(\widehat{NN})]$ ($\widehat{NN}$ = α-diimine; 3.2–3.3 Å),[19,20] probably caused by shorter Pt–C(1) bond lengths due to the weaker *trans* influence of the diimine ligands. The tilt angles between the aryl rings and the CCPtPP coordination plane range from 76 to 90° for the *cis* derivatives but are almost 90° for the two *trans*-configured analogues. Since 90° is the optimum value for steric reasons, this is remarkable. We have previously made a similar observation for related *cis*-configured (diimine)platinum complexes (angles around 70°) and have ascribed this effect to an optimisation of ligand-to-metal overlap in conjunction with a metal-mediated ligand-to-ligand interaction.[19] Such interactions seem to be absent for the *trans*-configured compounds.

Essential structural data marking the differences between *cis* and *trans* conformers are summarised in Table 4 together with DFT-calculated energies for possible isomers.

Table 4. Experimental and ADF/BP calculated structural data for complexes $[Pt(Ar)_2(PEt_3)_2]$.

	Exp. structure from single-crystal XRD	Lowest-energy structure[a]/ stabilisation energy [kcal mol^{-1}]
$[Pt(Ph)_2(PEt_3)_2]$	*cis* (173 K)	*cis*/10.7
$[Pt(2\text{-}Tol)_2(PEt_3)_2]$ (*syn*)	*cis-syn* (293 K)[b]	*cis-syn*/6.2
$[Pt(2\text{-}Tol)_2(PEt_3)_2]$ (*anti*)	*cis-anti* (293 K)[b]	*cis-anti*/5.8
$[Pt(3\text{-}Tol)_2(PEt_3)_2]$ (*syn*)	*cis-syn* (173 K)	*cis-syn*/3.5
$[Pt(3\text{-}Tol)_2(PEt_3)_2]$ (*anti*)	–	*cis-anti*/3.5
$[Pt(4\text{-}Tol)_2(PEt_3)_2]$	*cis* (173 K)	*cis*/3.0
$[Pt(Xyl)_2(PEt_3)_2]$	*trans* (173 K)	*trans*/4.7
$[Pt(Mes)_2(PEt_3)_2]$	*trans* (173 K)	*trans*/7.3

[a] Calculated data for $[Pt(Ar)_2(PMe_3)_2]$ model systems, stabilisation energy calculated as the energy difference between the highest and lowest bonding energies of the corresponding *cis* and *trans* isomers. [b] Data for *cis*-$[Pt(2\text{-}Tol)_2(PEt_3)_2]$ (*cis-syn*: monoclinic $P2_1/n$, *cis-anti*: monoclinic $P2_1/c$) from ref.[14]

The ADF/BP calculated ground-state molecular structures agree fully with the experimental structures The *syn* isomer was calculated to be slightly more stable (1 kcal mol^{-1}) for the *cis*-2-Tol complex, which is in agreement with the observed ratio of *syn*/*anti* stereoisomers of approximately 2:1 in solution (see NMR). The calculated difference in bond energy for the *syn* and *anti* isomers of the 3-Tol derivative is negligible, which fully agrees with the approximate 1:1 ratio found in the low-temperature NMR spectra. The fact that we found the *syn* form for the 3-Tol derivative in the crystal structure determination can thus not be ascribed to its higher stability; it might instead be due to a higher tendency to crystallise.

Conclusions

The combination of structural and spectroscopic data with quantum chemical calculations on diarylplatinum complexes with triethylphosphane ligands has revealed that the borderline between *cis*- and *trans*-configured ground-state geometries is crossed when two *ortho*-methyl groups are introduced on the aryl ligands. Under the applied preparation conditions (high-temperature ligand exchange using the $[Pt(Ar)_2(DMSO)_2]$ precursor complexes) we found the selective formation of either the *cis* (Ph or Tol) or *trans* (Xyl or Mes) isomers. In case of the 2-Tol and the 3-Tol derivatives, the formation of a mixture of the *syn* and *anti* stereoisomers was observed. Detailed NMR experiments allowed the structural assignment of the individual isomers and within these experiments we did not observe any isomerisation reaction. Therefore, we postulate that our chosen reaction conditions are appropriate to obtain the thermodynamically most stable forms. The results of quantum chemical calculations are in excellent agreement with the findings, even in predicting the relative energies of *syn* or *anti* stereoisomers with relatively small energy differences.

Experimental Section

General: The precursor complexes $[Pt(Ar)_2(DMSO)_2]$ (Ar = Ph, 2-Tol, 3-Tol, 4-Tol, 2,6-Xyl or Mes) were prepared according to literature methods.[15,18] Triethylphosphane was obtained from Aldrich. All reactions were carried out under argon in dry and distilled analytical-grade solvents. One-dimensional ^1H, $^{13}C\{^1H\}$, $^{31}P\{^1H\}$, and $^{195}Pt\{^1H\}$ NMR spectra were recorded with a Bruker DPX-300 NMR spectrometer (^1H: 300.13; ^{13}C: 75.47; ^{31}P: 121.49; ^{195}Pt: 64.52 MHz). Chemical shifts are relative to the internal chloroform peak at δ = 7.26 ppm for ^1H and δ = 77.0 ppm for ^{13}C, external 85% H_3PO_4 for ^{31}P and Na_2PtCl_6 in D_2O for ^{195}Pt. A 90° pulse was used in every case. NMR measurements for the assignment of the *syn* and *anti* conformations of $[Pt(2\text{-}Tol)_2(PEt_3)_2]$ were carried out with a Bruker DPX 400 spectrometer (^1H: 400.13 MHz; ^{195}Pt: 86.01 MHz; ^{13}C: 100.3 MHz) in $CDCl_3$ at 303(1) K; for $[Pt(3\text{-}Tol)_2(PEt_3)_2]$ these measurements were performed in CD_2Cl_2 at 223(5) or 193(5) K; chemical shifts were referenced to external TMS (^1H, ^{13}C) or K_2PtCl_6 (Ξ = 21.496784 MHz, ^{195}Pt). The assignment of ^{13}C and ^{195}Pt resonances was obtained from two-dimensional gradient selected (gs) $^1H,^{13}C$ HMQC and HMBC and $^1H,^{195}Pt$ HMQC spectra. Conformational assignments and the analysis of dynamic properties were derived from two-dimensional ^1H gs-NOESY NMR spectra using mixing times of between 500 and 750 ms. All 2D NMR spectra were obtained by using standard pulse sequences from the Bruker pulse program library.

Synthesis of the Complexes $[Pt(Ar)_2(PEt_3)_2]$: An excess of triethylphosphane (1 mmol) was added to a stirred toluene (20 mL) solution of $[Pt(Ar)_2(DMSO)_2]$ (Ar = Ph, 2-Tol, 3-Tol, 4-Tol, Xyl, Mes; typically 0.28 mmol). The mixture was stirred with refluxing for 24 h. The solvent, DMSO and the excess of PEt_3 were distilled off and the residue washed with cold pentane. The colourless products were dried in vacuo. Recrystallisation of the products from warm pentane gave colourless crystals. Yields and elemental analyses are given in Table 5, and full NMR spectroscopic data in Tables 6, 7 and 8.

Table 5. Yields and analytical data of complexes $[Pt(Ar)_2(PEt_3)_2]$.

Ar	Yield [mg]	Yield [%]	Calculated [%]	Found [%]
Ph	105	64	C 49.22, H 6.89	C 50.01, H 6.90
2-Tol	167	97	C 50.89, H 7.23	C 50.93, H 7.28
3-Tol	168	98	C 50.89, H 7.23	C 50.90, H 7.24
4-Tol	165	96	C 50.89, H 7.23	C 50.94, H 7.27
Xyl	154	86	C 52.41, H 7.54	C 52.53, H 7.58
Mes	161	86	C 53.80, H 7.83	C 53.83, H 7.83

Crystallography: Single crystals of $[Pt(Ar)_2(PEt_3)_2]$ (Ar = Ph, 3-Tol, 4-Tol, 2,6-Xyl or Mes) were obtained by slow evaporation of the solvent from saturated solutions in CH_2Cl_2 or pentane. The X-ray data of these complexes were collected at 173(2) K with a Siemens P4 or P3 diffractometer, using graphite-monochromated Mo-K_α radiation (λ = 0.71073 Å) and employing Wyckoff scans. The structures for Ar = Xyl or Mes were solved by direct methods; for all others the Patterson method was employed, in each case using the SHELXTL package,[22] while refinement was carried out with SHELXL97 employing full-matrix least-squares methods on F^2 with $F_o^2 \geq 2\sigma(F_o^2)$.[23] All non-hydrogen atoms were refined aniso-

Table 6. ^1H NMR spectroscopic data of complexes $[Pt(Ar)_2(PEt_3)_2]$.[a]

Ar	H(2)	H(6)	H(3)	H(5)	H(4)	δ ($J_{H,Pt}$) $CH_3(o)$	$CH_3(m)$	$CH_3(p)$	CH_2(Et)	CH_3(Et)
Ph	7.31 (55.5)	7.31 (55.5)	6.84 (21.6)	6.84 (21.6)	6.63	–	–	–	1.50	1.08
2-Tol (*syn*)[b]	–	7.4 (56.0)	6.77	6.67	6.77	2.45 (5.7)	–	–	1.47	1.07
2-Tol (*anti*)[b]	–	7.37 (54.5)	6.77	6.67	6.77	2.60 (5.9)	–	–	1.47	1.07
3-Tol (303 K)	7.16 (56.7)	7.10 (56.8)	–	6.74 (25.2)	6.46	–	2.15	–	1.48	1.07
3-Tol (193 K)	7.00 (br)	6.95 (br)	–	6.63/ 6.60	6,33 (br)	–	1.98/ 2.01	–	1.27 (br)	0.88 (br)
4-Tol	7.16 (56.9)	7.16 (56.9)	6.68	6.68	–	–	–	2.10	1.51	1.07
Xyl	–	–	6.80	6.80	6.80	2.60 (5.1)	–	–	1.32	0.89
Mes	–	–	6.64	6.64	–	2.54 (4.7)	–	2.17	1.29	0.89

[a] Chemical shifts in ppm ($J_{H,Pt}$ in Hz), as measured in CD_2Cl_2. [b] Measured in $CDCl_3$.

Table 7. ^{13}C NMR spectroscopic data of complexes $[Pt(Ar)_2(PEt_3)_2]$.[a]

Ar	C(1)	C(2)	C(6)	C(3)	C(5)	δ ($J_{C,Pt}$) C(4)	CH_3(*o*)	CH_3(*p*)	CH_2(Et)	[b]	CH_3(Et)
Ph	155.1	127.1	127.1	136.8	136.8	121.0	–	–	15.9		8.2
	(878.9)	(63.5)	(63.5)	(34.1)	(34.1)	(12.3)			(26.4)	(29.1)	(17.6)
2-Tol (*syn*)	162.5	127.6	123.8	142.2	135.8	121.0	27.5	–	15.8		8.0
	(844.0)	(43.0)	(62.4)	(25.4)	(24.3)	(9.6)	(74.6)				
2-Tol (*anti*)	161.4	128.2	123.7	142.6	136.8	120.9	25.9	–	15.8		8.0
	(832.2)	(40.0)	(62.7)	(20.4)	(37.9)	(9.2)	(67.3)				
3-Tol (303 K)[c]	164.4	137.1	133.4	135.2	126.3	121.2		21.7	15.4		7.7
	(812)	(34.6)	(32.9)	(63.4)	(66.1)	(11.5)		[d]	(21.8)		(17.4)
3-Tol (193 K)[c]	166.6/	136.9/	133.0/	135.6	126.3	121.0/	21.6/		14.6		8.1
	166.5	137.2	133.1	(br)	(br)	121.0	21.6		(br)		
4-Tol	160.8	127.7	127.7	135.8	135.8	129.1	–	20.9	15.6		8.2
	(1090)	(66.2)	(66.2)	(35.4)	(35.4)	(5.8)			(25.6)	(28.6)	(17.7)
Xyl	160.2	125.2	125.2	145.0	145.0	121.9	26.6	–	15.0		7.83
	(591.1)	(24.9)	(24.9)				(55.5)		(32.9)	(41.0)	(16.24)
Mes	155.5	126.3	126.3	144.7	144.7	131.1	26.4	20.8	15.0		7.87
	(536.0)						(59.0)		(33.5)	(39.6)	(17.7)

[a] Chemical shifts in ppm ($J_{C,Pt}$ in Hz), as measured in $CDCl_3$. [b] Further coupling $^2J_{CH_2,P}$ (Hz). [c] In CD_2Cl_2. [d] *m*CH_3.

Table 8. ^{31}P NMR and ^{195}Pt NMR spectroscopic data of complexes $[Pt(Ar)_2(PEt_3)_2]$.[a]

Ar	$\delta_{^{31}P}$	$\delta_{^{195}Pt}$
Ph	5.4 (t, $^1J_{P,Pt}$ = 1775 Hz)	–4568 (t, $^1J_{P,Pt}$ = 1790 Hz)[b]
2-Tol (*syn*)	0.8 (t, $^1J_{P,Pt}$ = 1751 Hz)	–4471 (t, $^1J_{P,Pt}$ = 1751 Hz)
2-Tol (*anti*)	1.0 (t, $^1J_{P,Pt}$ = 1739 Hz)	–4466 (t, $^1J_{P,Pt}$ = 1739 Hz)
3-Tol (303 K)	3.9 (t, $^1J_{P,Pt}$ = 1754 Hz)	–4570 (t, $^1J_{P,Pt}$ = 1764 Hz)
3-Tol (193 K)[c]	2.42 ($^1J_{P,Pt}$ = 1754 Hz)	–4587 (t, $^1J_{P,Pt} \approx$ 1.77 kHz)
	2.45 ($^1J_{P,Pt}$ = 1754 Hz)	–4589 (t, $^1J_{P,Pt} \approx$ 1.77 kHz)
4-Tol	4.0 (t, $^1J_{P,Pt}$ = 1762 Hz)	–4566 (t, $^1J_{P,Pt}$ = 1780 Hz)
Xyl	1.1 (t, $^1J_{P,Pt}$ = 2845 Hz)	–4311 (t, $^1J_{P,Pt}$ = 2848 Hz)
Mes	1.8 (t, $^1J_{P,Pt}$ = 2841 Hz)	–4306 (t, $^1J_{P,Pt}$ = 2841 Hz)

[a] Chemical shifts in ppm ($J_{P,Pt}$ in Hz), as measured in $CDCl_3$. [b] Measured in $(CD_3)_2CO$. [c] In CD_2Cl_2.

tropically, including the disordered C atoms of the ethyl groups in the compounds Ar = 3-Tol or Mes. Hydrogen atoms were introduced using appropriate riding models. An empirical absorption correction was performed using ψ-scans. CCDC-266186 for $[Pt(Ph)_2(PEt_3)_2]$, -266187 for $[Pt(3\text{-}Tol)_2(PEt_3)_2]$, -266188 for $[Pt(4\text{-}Tol)_2(PEt_3)_2]$, -266189 for $[Pt(2,6\text{-}Xyl)_2(PEt_3)_2]$ and -266190 for $[Pt(Mes)_2(PEt_3)_2]$ contain the supplementary crystallographic data for this paper. These data can be obtained free of charge from The Cambridge Crystallographic Data Centre via www.ccdc.cam.ac.uk/data_request/cif.

Quantum Chemical Calculations: Ground-state electronic structure calculations were performed by density-functional theory (DFT) methods using the ADF2004.01 program package.[24] Nuclear spin-spin coupling constants were calculated with the CPL module[25] within ADF2004.01. The calculations were performed on the model systems $[Pt(Ar)_2(PMe_3)_2]$ due to the size of the $[Pt(Ar)_2(PEt_3)_2]$ complexes. Slater-type orbital (STO) basis sets of triple-ζ quality with one polarisation function (TZ2P)[24b] for Pt and two polarisation functions (TZP)[24b] for the remaining atoms were employed for geometry optimisation. The inner shells were represented by the frozen-core approximation (1s for C, 2p for P and 1s–4d for Pt were kept frozen). Core electrons were included for the calculation of NMR parameters, and here the quadruple-ζ with four polarisation functions (QZ4P)[24b] basis set was used for Pt. The calculations were carried out with the functional including Becke's gradient correction[26] to the local exchange expression in conjunction with Perdew's gradient correction[27] to the local correlation (BP86). The scalar relativistic (SR) zero-order regular approximation (ZORA) was used within this study. The energy barriers of *syn*/*anti* isomerisation within $[Pt(2\text{-}Tol)_2(PMe_3)_2]$ and $[Pt(3\text{-}Tol)_2(PMe_3)_2]$ model complexes were calculated as the lowest energy rotation barrier associated with the rotation of one 2-Tol or 3-Tol group, respectively.

Acknowledgments

Dr. M. Bader and Dr. M. Niemeyer (University of Stuttgart) are thanked for collecting single-crystal XRD data. Support for this work under the Indo-German bilateral program from the BMBF (Project No. IND 99/060) and the COST D14 action is also acknowledged. We are also grateful for a loan of K_2PtCl_4 by Johnson Matthey. S. Z. also acknowledges financial support by the Grant Agency of the Academy of Sciences of the Czech Republic (grant 1ET400400413).

[1] F. R. Hartley, *The Chemistry of Platinum and Palladium*, John Wiley & Sons, New York, **1973**.
[2] J. N. Harvey, K. M. Heslop, A. G. Orpen, P. G. Pringle, *Chem. Commun.* **2003**, 278–279 and references cited therein.
[3] G. K. Anderson, R. J. Cross, *Chem. Soc. Rev.* **1980**, *9*, 185–215.
[4] G. A. Petsko, *Nature* **1995**, *377*, 580–581.
[5] P. J. Sadler, *Adv. Inorg. Chem.* **2000**, *49*, 183–306.
[6] *Cisplatin – Chemistry and Biochemistry of a Leading Anticancer Drug* (Ed.: B. Lippert), 1st ed., Helvetica Chimica Acta (Zürich), Wiley-VCH (Weinheim), **1999**.
[7] J. Chatt, R. G. Wilkins, *J. Chem. Soc.* **1952**, 273–278.
[8] J. Chatt, R. G. Wilkins, *J. Chem. Soc.* **1952**, 4300–4306.
[9] J. Chatt, B. L. Shaw, *J. Chem. Soc.* **1959**, 4020–4033.
[10] T. G. Appleton, M. A. Bennett, *Inorg. Chem.* **1978**, *3*, 738–747.
[11] R. Romeo, M. R. Plutino, L. M. Scolaro, S. Stoccoro, *Inorg. Chim. Acta* **1997**, *265*, 225–233.
[12] P. Power, *J. Organomet. Chem.* **2004**, *689*, 3904–3919.

[13] M. C. Biagini, M. Ferrari, M. Lanfranchi, L. Marchio, M. A. Pellinghelli, *J. Chem. Soc., Dalton Trans.* **1999**, 1575–1580.
[14] A. L. Rieger, G. B. Carpenter, P. H. Rieger, *Organometallics* **1993**, *12*, 842–847.
[15] A. Knödler, T. Schurr, A. Klein, W. Kaim, V. K. Jain, K.-W. Klinkhammer, D. Gudat, S. Záliš, *Organometallics* **2005**, *24*, 4125–4131.
[16] M. Hashemi, M. Rashidi, *J. Organomet. Chem.* **2005**, *690*, 982–989.
[17] A. T. Hutton, P. G. Pringle, B. L. Shaw, *J. Chem. Soc., Dalton Trans.* **1985**, 1677–1682.
[18] C. Eaborn, K. Kundu, A. Pidcock, *J. Chem. Soc., Dalton Trans.* **1981**, 933–938.
[19] A. Klein, J. van Slageren, S. Záliš, *Eur. J. Inorg. Chem.* **2003**, 1917–1938.
[20] W. Kaim, A. Klein, *Organometallics* **1995**, *14*, 1176–1186.
[21] N. Mintcheva, Y. Nishihara, M. Tanabe, K. Hirabayashi, A. Mori, K. Osakada, *Organometallics* **2001**, *20*, 1243–1246.
[22] G. M. Sheldrick, *SHELXTL*, Bruker Analytical X-ray Systems, Madison, Wisconsin, USA, **1998**.
[23] G. M. Sheldrick, *SHELXL-97: A program for Crystal Structure Determination*, Universität Göttingen, Göttingen, Germany, **1997**.
[24] a) G. te Velde, F. M. Bickelhaupt, S. J. A. van Gisbergen, C. Fonseca Guerra, E. J. Baerends, J. G. Snijders, T. Ziegler, *J. Comput. Chem.* **2001**, *22*, 931–967; b) ADF2004.01, SCM, Theoretical Chemistry, Vrije Universiteit, Amsterdam, The Netherlands, http://www.scm.com.
[25] a) J. Autschbach, T. Ziegler, *J. Chem. Phys.* **2000**, *113*, 936–947; b) J. Autschbach, T. Ziegler, *J. Chem. Phys.* **2000**, *113*, 9410–9418.
[26] A. D. Becke, *Phys. Rev. A* **1988**, *38*, 3098–3100.
[27] J. P. Perdew, *Phys. Rev. B* **1986**, *33*, 8822–8824.

Received: March 23, 2005
Published Online: September 5, 2005

